

Carbon Dioxide Hydrogenation

International Edition: DOI: 10.1002/anie.201610166
German Edition: DOI: 10.1002/ange.201610166CO₂-to-Methanol Hydrogenation on Zirconia-Supported Copper Nanoparticles: Reaction Intermediates and the Role of the Metal–Support Interface**

Kim Larmier, Wei-Chih Liao, Shohei Tada, Erwin Lam, René Verel, Atul Bansode, Atsushi Urakawa, Aleix Comas-Vives,* and Christophe Copéret*

Abstract: Methanol synthesis by CO₂ hydrogenation is a key process in a methanol-based economy. This reaction is catalyzed by supported copper nanoparticles and displays strong support or promoter effects. Zirconia is known to enhance both the methanol production rate and the selectivity. Nevertheless, the origin of this observation and the reaction mechanisms associated with the conversion of CO₂ to methanol still remain unknown. A mechanistic study of the hydrogenation of CO₂ on Cu/ZrO₂ is presented. Using kinetics, in situ IR and NMR spectroscopies, and isotopic labeling strategies, surface intermediates evolved during CO₂ hydrogenation were observed at different pressures. Combined with DFT calculations, it is shown that a formate species is the reaction intermediate and that the zirconia/copper interface is crucial for the conversion of this intermediate to methanol.

The catalytic hydrogenation of CO₂ to methanol is a key process in a sustainable methanol-based economy.^[1] While copper-based catalysts are highly active for this transformation,^[2] their activity and selectivity strongly depends on the support and/or promoters. Understanding the copper–support interaction—particularly its effect on the activity and product selectivity—has been a very intensive field of research over the last decade. While the reaction mechanisms and the nature of the active sites on Cu/ZnO systems have been extensively investigated,^[3] copper supported on zirconia (and related materials) also exhibits high activity and selectivity in CO₂ hydrogenation to methanol [Eq. (1)] by minimizing the formation of CO, a byproduct often resulting from the competitive reverse water-gas shift reaction [Eq. (2)].^[4]



Although the Cu/ZrO₂ interface was proposed to play a key role in the selective formation of methanol,^[4c,e-g] the active site and the reaction mechanism, including the role of the interface on methanol selectivity, are still not understood. In fact, mechanistic investigations using diffuse reflectance IR Fourier transform spectroscopy (DRIFTS) led to opposite conclusions: formate is an intermediate in methanol formation^[4c,d] versus CO₂ is first reduced to CO that is in turn hydrogenated to methanol through a carboxyl intermediate.^[4f]

Herein, by using a combined experimental and computational approach on realistic models, we investigated the reaction mechanism of CO₂ hydrogenation to methanol on a Cu/ZrO₂ catalyst. Kinetic investigation, in situ and ex situ spectroscopies—FTIR and NMR—together with isotopic labeling and computational modeling, showed that methanol is a primary product formed by the hydrogenation of formate as a reaction intermediate.

First, narrowly dispersed copper nanoparticles supported on monoclinic zirconia were prepared by a molecular approach.^[5] Grafting of [Cu(O'Bu)]₄ on the surface hydroxyl groups of the support (Supporting Information, Figures S1 and S2, Scheme S1) followed by the treatment under H₂ at 500 °C for 5 h^[6] yielded small and narrowly distributed copper nanoparticles (2.2 ± 0.5 nm with 0.8 wt % copper loading; Supporting Information, Figure S3a). Using the same method, we also prepared a Cu/SiO₂ catalyst as a mimic of pure copper particles in order to probe their specific reactivity. This sample contains copper particles with a size distribution of 2.1 ± 0.5 nm with a 2.3 wt % copper loading (Supporting Information, Figure S3b). The catalytic activities of the samples were measured in a fixed-bed flow reactor at 230 °C and 25 bars (H₂/CO₂ molar ratio 3:1) under steady-state conditions (Supporting Information, Figure S4). For each sample, the contact time was increased by decreasing the volumetric flow rate (*Q*) of the feed gas. Figure 1a shows the evolution of the formation rates of methanol and CO as a function of the contact time. For both catalysts the rates strongly depend on the contact time. Extrapolations of the initial rates to zero conversion (zero contact time) for the two catalysts (Figure 1b) clearly show a strictly positive initial rate of formation for both CO and methanol, which indicates that they are both primary products. Thus, the intermediacy of CO in the formation of methanol is unlikely. Second, while the rate of CO formation is of the same order of magnitude for

[*] Dr. K. Larmier, W.-C. Liao, Dr. S. Tada, E. Lam, Dr. R. Verel, Dr. A. Comas-Vives, Prof. C. Copéret
Department of Chemistry and Applied Biosciences, ETH Zürich
Vladimir-Prelog Weg 1–5, 8093 Zürich (Switzerland)
E-mail: comas@inorg.chem.ethz.ch
ccoperet@inorg.chem.ethz.ch

Dr. A. Bansode, Prof. A. Urakawa
Institute of Chemical Research of Catalonia (ICIQ)
The Barcelona Institute of Science and Technology
Av. Paisos Catalans 16, 43007 Tarragona (Spain)

[**] This work was presented at the CO₂ Catalysis Conference, April 2016, Albufeira, Portugal.

Supporting information and the ORCID identification number(s) for the author(s) of this article can be found under <http://dx.doi.org/10.1002/anie.201610166>.

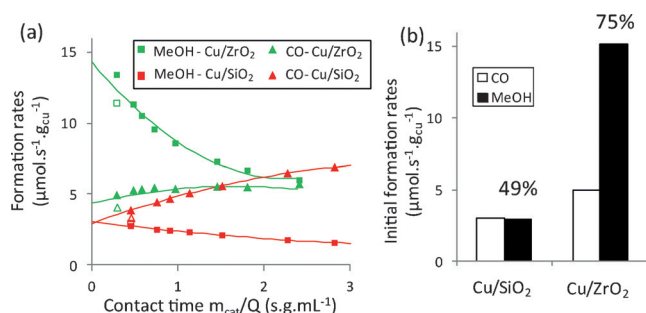


Figure 1. a) Rates of formation of CO and methanol with contact time on Cu/ZrO₂ and Cu/SiO₂ measured in a flow reactor at 230 °C and 25 bars (H₂/CO₂ = 3:1). Unfilled symbols correspond to activity when the first data point was repeated after 40 h of reaction, showing slow deactivation. CO₂ conversion was kept between 0.5 and 6%. b) Extrapolated rates of formation at zero conversion. The selectivity to methanol is indicated.

both catalysts, the rate of methanol formation is dramatically increased on Cu/ZrO₂. Thus, CO formation likely occurs on the copper surface, while methanol is formed at a much higher rate when both copper and zirconia are present. As a result, Cu/ZrO₂ displays much higher initial activity and methanol selectivity (15 μmol.s⁻¹.g_{Cu}⁻¹, 75%) than Cu/SiO₂ (2.6 μmol.s⁻¹.g_{Cu}⁻¹, 49%). On Cu/SiO₂, the rate of CO formation increases with contact time while the opposite is observed for methanol, which is likely due to partial methanol decomposition into CO. On Cu/ZrO₂, similar trends are observed for CO formation. However, the decrease in methanol formation rate with contact time is much sharper, which is likely due to inhibition of methanol formation by reaction products, such as water, or methanol itself. Both molecules are basic and strongly bind zirconia, suggesting that the active sites may involve Lewis acidic zirconium atoms. This inhibition is essentially reversible, as going back to a low contact time mostly restores the activity. A slight deactivation occurs over 40 h on stream (empty data point in Figure 1a). Overall, the methanol selectivity strongly decreases with contact time and conversion on both catalysts (Supporting Information, Figure S4c,d).

To obtain information about surface reaction intermediates, CO₂ hydrogenation on Cu/ZrO₂ was investigated by in situ DRIFTS at 230 °C under varying pressures (1–20 bars). The IR spectrum of the pristine catalyst shows only OH stretching frequencies at 3774 and 3670 cm⁻¹ (Supporting Information, Figure S5a). After contacting pre-reduced Cu/ZrO₂ with a H₂/CO₂ mixture (3:1) at 230 °C and 1 bar, features appeared in the ν(CH) (Supporting Information, Figure S6a) and ν(CO) regions (Supporting Information, Figure S6b). The main broad ν(OCO) features at 1593 cm⁻¹ can be attributed to carbonate or bicarbonate (CO₃* or (CO₃H)*),^[7] and the bands at 2978, 2878, 2736, 1567, and 1387 cm⁻¹ are characteristic of formate species adsorbed on zirconia (HCOO-ZrO₂; Supporting Information, Section 5).^[4d,7,8] The presence of formate on copper cannot be excluded, as a characteristic band at 1357 cm⁻¹ is also observed.^[4d] Increasing the reaction pressure to 5 bars (Supporting Information, Figure S6a,b), or higher pressures,

resulted in the appearance of new features at 2942 and 2828 cm⁻¹, and characteristic C-O stretching frequencies at 1154 and 1049 cm⁻¹ that were attributed to methoxy adsorbed on zirconia.^[4f,7] Interestingly, when pure zirconia was used, only carbonate, bicarbonate, and formate species were observed (Supporting Information, Figure S6). This suggests that the presence of copper on zirconia is responsible for the formation of methoxy species.

We subsequently investigated the nature of the reaction intermediates by solid-state NMR spectroscopy. Note that NMR will preferably provide information about species adsorbed on zirconia, as adsorbed species on metallic copper can suffer from severe signal broadening (Supporting Information, Section 5). Cu/ZrO₂ was contacted with a H₂/¹³C mixture (3:1) at 230 °C for 12 h in a high-pressure glass reactor at 1 and 5 bars. After cooling down to room temperature, the gas phase was evacuated and the solid was analyzed by solid-state NMR. The ¹H-¹³C heteronuclear correlation (HETCOR) spectrum of the sample after reaction at 1 bar is shown in Figure 2a. The correlation of the ¹³C NMR chemical shift at 168 ppm to the ¹H NMR signal at 8.4 ppm is consistent with the presence of formate species; the line broadening in the ¹H dimension suggests the presence of formate in different chemical environments. After reaction at 5 bars (Figure 2b), an additional correlation is observed at δ(¹³C) = 51 ppm and δ(¹H) = 4.0 ppm, which is consistent with the formation of surface methoxy species. The NMR data are in agreement with what is observed by in situ DRIFTS. However, the absence of carbonates in both ex situ NMR or IR experiments (Supporting Information, Figure S5b,c) shows that these species are weakly adsorbed.

On the contrary, the formate and methoxy species are strongly adsorbed and remain on the surface even after evacuation under high vacuum. Finally, when similar experiments were performed on pure zirconia, formate species were observed (Supporting Information, Figure S16) but no methoxy, as previously observed by in situ DRIFTS. On Cu/SiO₂, IR spectroscopy shows (Supporting Information, Figure S13) the formation of formate, which was identified by bands at 2937, 2858, and 1544 cm⁻¹. The presence of formate could be confirmed by the observation of a very broad and weak feature at 168 ppm in cross-polarization magic-angle spinning (CP-MAS). No methoxy could be observed (Supporting Information, Figures S14 and S15). Thus, copper particles by themselves, or the pure support, are not able to generate significant amounts of methoxy from formate under these conditions (230 °C; 5 bars).

To evaluate whether or not formate is a reaction intermediate in methanol synthesis, additional isotopic labeling experiments were carried out. First, we selectively prepared ¹³C-labeled formate adsorbed on the surface (H¹³COO*) by reacting Cu/ZrO₂ with a H₂/¹³CO₂ mixture (3:1) at 1 bar and 230 °C (Figure 2a). In a second step, following cooling down to room temperature and evacuation of the gas phase (10⁻⁴ mbar, 2 h), the sample was treated with 5 bars of D₂ at 230 °C for 12 h. MAS-NMR and IR spectra of the resulting solid were recorded (Figure 2c; Supporting Information, Figure S5d). A ¹H-¹³C CP-MAS NMR spectrum shows two signals at 168 and 51 ppm, attributed to formate and methoxy

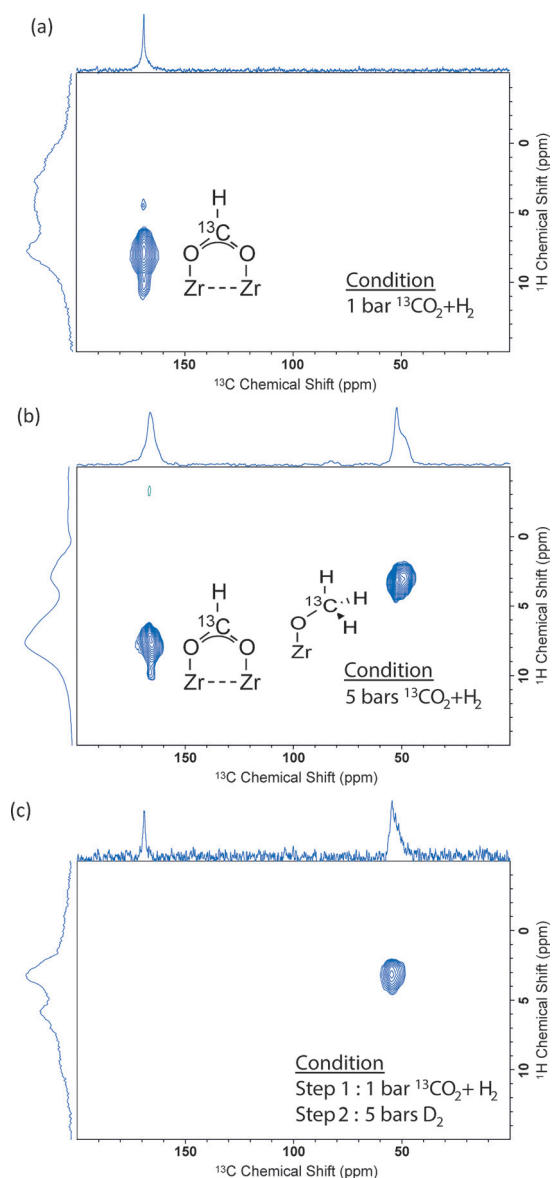
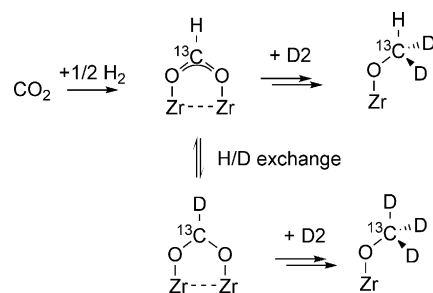


Figure 2. Ex situ MAS-NMR ^1H - ^{13}C HETCOR spectra of Cu/ZrO_2 reacted with $\text{H}_2/^{13}\text{CO}_2$ (3:1) at 230°C for 12 h at a) 1 bar or b) 5 bars. c) Ex situ MAS-NMR ^1H - ^{13}C HETCOR spectrum of Cu/ZrO_2 after two-step hydrogenation of $^{13}\text{CO}_2$: Step 1) hydrogenation at 1 bar, 230°C , 12 h; Step 2) deuteration at 5 bars, 230°C , 12 h. For HETCOR experiments, ramp cross polarization (^1H - ^{13}C) was used with a contact time of 0.5 ms. The recycle delay was 1 s. External projections of the 1D ^{13}C and ^1H spectra are applied in all spectra.

species, respectively. In this experiment, the formate initially present on the surface after the first step (treatment by $^{13}\text{CO}_2$ and H_2) is the only source of ^{13}C and ^1H , so that the methoxy surface species must be formed from deuteration of the initial formate species, supporting its involvement as a reaction intermediate in methanol formation. To further characterize the nature of the intermediates adsorbed on the surface, and the isotopic source of the methoxy species, the sample was extracted and analyzed by solution state NMR; it was divided in two fractions prior to extraction. The first fraction was extracted with D_2O and a ^1H solution NMR spectrum was

recorded (Supporting Information, Figure S18), and the second fraction was extracted with H_2O and a ^2D solution NMR spectrum was recorded (Supporting Information, Figure S19). The ^1H spectrum shows a doublet of pentet centered at 3.12 ppm, with coupling constants $J(^1\text{H}$ - $^{13}\text{C}) = 141$ Hz and $J(^1\text{H}$ - $^2\text{D}) = 1.7$ Hz consistent with the formation of $^{13}\text{CHD}_2\text{OD}$. The ^2D spectrum shows a doublet centered at 3.15 ppm ($J(^2\text{D}$ - $^{13}\text{C}) = 21$ Hz), but did not show additional ^1H - ^2D coupling, thus indicating that the most abundant species correspond to fully deuterated methanol $^{13}\text{CD}_3\text{OH}$. This is also consistent with the absence of a formate signal in the ^1H - ^{13}C HETCOR spectrum (Figure 2c). Taken together, the results suggest that the formate can exchange hydrogen with deuterium prior to deuteration, indicating that the formation of methoxy species is slower than the H/D exchange of formate, as shown in Scheme 1. IR spectroscopy



Scheme 1. Reaction scheme derived from the spectroscopic measurements.

also reveals a high degree of H/D exchange upon contact of the sample with D_2 (Supporting Information, Figure S5d). Nonetheless, quantitative ^{13}C direct excitation NMR spectrum (Supporting Information, Figure S17) showed that a significant proportion of formate (deuterated or not) was converted into methoxy (about 60%). Furthermore, the 2D spectrum in solution allowed a rough estimation of the number of methanol molecules adsorbed on the surface prior to desorption to about 0.04 per nm^{-2} , which may be considered as an indication of the number of active sites. This number is close to the density of particles that can be estimated (0.01 per nm^{-2}), indicating a rather small number of active sites per copper particle (details in the Supporting Information). The NMR spectroscopic investigation shows that methoxy (methanol) is formed from formate species adsorbed on zirconia, as proposed earlier.^[4d] It also highlights the determining effect of pressure in the formation of the intermediates. We also show that both copper and zirconia are required for the reaction under such conditions. Thus, it can be proposed that the reaction takes place at the interface between zirconia and copper particles, as suggested in previous reports.^[4b,e]

To obtain molecular insights into the reaction mechanisms and possible involvement of this interface, we turned to DFT calculations. A model for the supported copper particles on zirconia and the potential interfacial active sites was constructed by depositing a Cu_{38} particle ($\varnothing = 0.8$ nm, truncated octahedron from *fcc* structure) on a *m*- ZrO_2 ($\bar{1}11$) slab, which

is the main termination exposed by monoclinic zirconia (Supporting Information, Figure S20).^[9] No significant deformation of the cluster was observed, consistent with the small change in the cohesive energy of the copper nanoparticle upon adsorption (-266 and -269 kJ mol^{-1} prior to and after adsorption, respectively). The zirconia slab model and a pristine (111) surface of *fcc* copper were also used for comparison. The adsorption modes of H_2 and CO_2 were assessed on these three model materials. In line with previous findings, the dissociative adsorption of H_2 is endoenergetic on the zirconia surface, either through heterolytic ($\Delta_r E = +57$ kJ mol^{-1}) or homolytic cleavage ($\Delta_r E = +241$ kJ mol^{-1}),^[9] while the dissociation of H_2 is exoenergetic by -40 kJ mol^{-1} on the Cu(111) facet.^[10] On the supported nanoparticle the dissociation is slightly more favorable than on the extended surface ($\Delta_r E = -50$ kJ mol^{-1}). CO_2 virtually does not bind the Cu(111) surface (-2 kJ mol^{-1} , Figure 3 a). On zirconia, CO_2

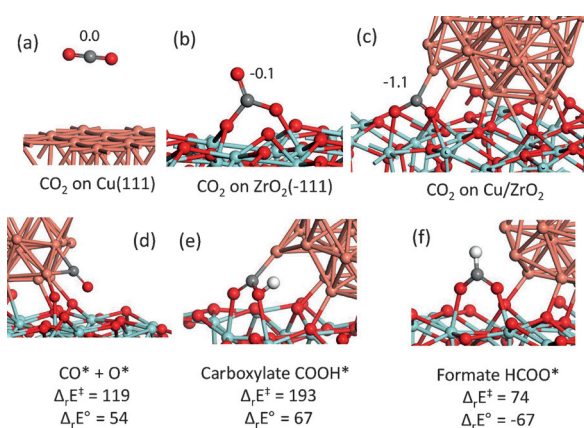


Figure 3. a–c) Optimized structures of CO_2 adsorbed on Cu(111) (a), on *m*- ZrO_2 ($\bar{1}\bar{1}\bar{1}$) (b), and at the interface between copper and zirconia (c). The Bader charge on CO_2 molecules is indicated. d–f) Structures of the possible intermediates at the interface between copper and zirconia: CO^* and O^* (d), carboxylate COOH^* (e), and formate HCOO^* (f). Activation barriers and formation enthalpy from adsorbed $\text{CO}_2 + \text{H}_2$ are given in kJ mol^{-1} . Atom key: zirconium (cyan), oxygen (red), copper (orange), carbon (gray), hydrogen (white).

adsorbs as a carbonate, or bicarbonate if a hydroxyl group is available, with adsorption energies of -65 and -70 kJ mol^{-1} , respectively (Figure 3 b; Supporting Information, Figure S21). However, we found a much more favorable adsorption mode of CO_2 at the interface between copper and zirconia ($\Delta_r E = -179$ kJ mol^{-1} , Figure 3 c), where CO_2 adopts a bent structure with the carbon atom bound to the copper particle surface, and the two oxygen atoms interact with Zr^{4+} Lewis acidic centers of the zirconia surface. A similar adsorption mode has been found for the adsorption of CO_2 on a Ni/ γ - Al_2O_3 interface.^[11] Bader charge analysis of this intermediate revealed a transfer of electron density from the copper particle to the CO_2 molecule (-1.1 compared to about 0 for CO_2 on Cu(111) and carbonates on ZrO_2), which is thus negatively charged and partially reduced. The positive charge is delocalized on the copper particle. This adsorption mode of CO_2 at the Cu/ ZrO_2 interface is therefore a very good

candidate for further reduction by H_2 , and was used as a starting point to calculate hydrogenation pathways.

We first examined the transformation of CO_2 into three commonly proposed intermediates:^[3a,12] 1) direct decomposition of CO_2 into CO (first step of the reverse water-gas shift reaction, Figure 3 d), 2) carboxyl intermediate (COOH^* , Figure 3 e), and 3) formate intermediate (HCOO^* , Figure 3 f). The activation barriers to form these intermediates from CO_2 chemisorbed at the interface and H_2 dissociated on the particle are given in Figures 3 d–f. Formation of the formate intermediate is the lowest energy pathway from all those evaluated, with an activation barrier of only 74 kJ mol^{-1} , compared to 119 and 193 kJ mol^{-1} for the formation of CO and COOH^* , respectively. It is also the most thermodynamically favorable pathway (-67 kJ mol^{-1}) in comparison with the formation of CO and COOH^* , which are endoenergetic by 54 and 67 kJ mol^{-1} , respectively. The whole pathway leading from CO_2 to methanol was thus calculated through the most favorable formate intermediate. The resulting energy and Gibbs free-energy diagrams are depicted in Figure 4, along with the main intermediates. Note that the highest point in the free-energy diagram (19 kJ mol^{-1}) lies lower than the transition states for the initial activation of CO_2 to CO^* (50 kJ mol^{-1}) or COOH^* (124 kJ mol^{-1}), confirming the relevance of the formate route as the most favorable pathway. From the formate—adsorbed on zirconia in close vicinity to the copper particle—transfer of an additional hydrogen atom from the copper particle can generate an acetal-like species $\text{H}_2\text{C}(\text{O})_2^*$, where both oxygen atoms are bound to two Zr^{4+} sites, with a low free-energy barrier (71 kJ mol^{-1}). The further hydrogenation of the acetal is the most energetically demanding step. A hydrogen atom is first transferred to one of the oxygen atoms to form H_2COOH^* ($\Delta_r G^\ddagger = 105$ kJ mol^{-1}). However, the relative energy barrier for this step is lower than that for the formation of CO^* and COOH^* intermediates. This high-energy intermediate is easily converted by the transfer of an additional hydrogen atom ($\Delta_r G^\ddagger = 52$ kJ mol^{-1}). In a concerted $\text{S}_{\text{N}}2$ -like step, the third C–H bond is formed while the C–OH bond is broken, leading to methoxy and hydroxyl groups adsorbed on the formally Zr^{4+} sites. Both can further undergo protonation by hydrogen transfer from the copper particle. Methanol and water are thus formed ($\Delta_r G^\ddagger = 52$ and 102 kJ mol^{-1} , respectively), and desorb with a desorption energy of -84 and -87 kJ mol^{-1} , respectively.

The lowest points in the diagram are formate and methoxy, and the calculated ^{13}C and ^1H chemical shifts are in good agreement with the experimental data (Supporting Information, Table S1 and Figure S22). Overall, the Gibbs free-energy diagram is rather flat, with an energy span of 151 kJ mol^{-1} . It is worth mentioning that it is significantly lower than what is found on a flat Cu(111) surface (267 kJ mol^{-1} ; Supporting Information, Figure S23) or even stepped Cu(211) facets (over 200 kJ mol^{-1} calculated at the GGA-PBE level of theory).^[3a]

In conclusion, we show that CO_2 can be transformed into carbonate or bicarbonate, formate, and methoxy, upon adsorption and hydrogenation on zirconia-supported copper nanoparticles. Experimentally, carbonate and bicarbonate

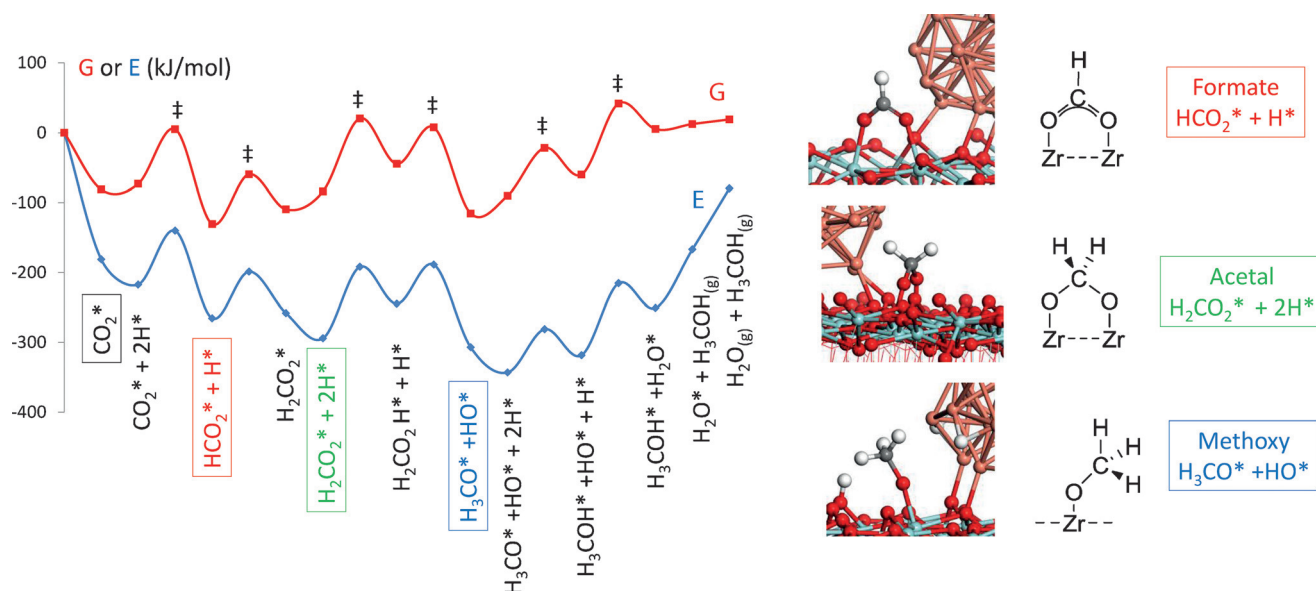


Figure 4. Energy and standard Gibbs free-energy pathway at 473 K calculated for the hydrogenation of CO₂ to methanol at the Cu/ZrO₂ interface. Energetics are referenced to the Cu/ZrO₂ model and CO₂(g) + 3 H₂(g). The lowest intermediates in Gibbs free energy are shown on the right.

can only be observed under in situ conditions, which is consistent with the low calculated adsorption energies (about -70 kJ mol^{-1}), in contrast with the strong adsorption of formate and methoxy species. The acetal, which is the next most stable intermediate, was not observed under the described reaction conditions. In fact, calculations show that it lies about 20 kJ mol^{-1} higher in energy than the formate, with a low formate–acetal interconversion barrier of about 70 kJ mol^{-1} . Thus both intermediates can be in equilibrium (in favor of the formate). This interconversion is consistent with the observed H/D exchange of the formate intermediate (Scheme 1). Overall, the formate species is a key and observable reaction intermediate in the hydrogenation of CO₂ to methanol on Cu/ZrO₂. The proposed mechanism is reminiscent of that recently proposed for a ruthenium molecular catalyst, bridging the gap between molecular and heterogeneous catalysis.^[13] The obtained results clearly point to the crucial molecular role of the interface between the copper particles and zirconia,^[4b,e] paving the road toward a more rational design of efficient heterogeneous CO₂ hydrogenation catalysts.

Acknowledgements

This work was conducted in the frame of the Synergia project (SNF project IZK0Z2_160957). K.L., E.L., and S.T. were supported by the SCCER—Heat and Energy Storage program, W.C.L. by SNF (200020_149704), and A.C.V. by the SNF funding program (Ambizione Project PZ00P2_148059). K.L. thanks the ETH Career Seed Grant SEED-21 16-2. S.T. also thanks the Japan Society for the Promotion of Science for a fellowship (JSPS, No. 15J10157). A.B. and A.U. acknowledge Generalitat de Catalunya for financial support through the CERCA Programme and MINECO, Spain for financial support (CTQ2012-34153) and for support through Severo

Ochoa Excellence Accreditation 2014–2018 (SEV-2013-0319). The authors thank Dr. T. C. Ong (ETHZ) for many useful discussions and the quantitative ¹³CSSNMR measurement, T.-H. Lin (ETHZ) for his precious help in using the high-pressure glass-reactor, and J. J. Corral (ICIQ) for assistance during high-pressure DRIFTS measurements.

Conflict of interest

The authors declare no conflict of interest.

Keywords: CO₂ hydrogenation · copper · density functional theory · solid-state NMR · zirconia

How to cite: *Angew. Chem. Int. Ed.* **2017**, *56*, 2318–2323
Angew. Chem. **2017**, *129*, 2358–2363

- [1] A. Goepfert, M. Czaun, J. P. Jones, G. K. S. Prakash, G. A. Olah, *Chem. Soc. Rev.* **2014**, *43*, 7995–8048.
- [2] M. Saito, T. Fujitani, M. Takeuchi, T. Watanabe, *Appl. Catal. A* **1996**, *138*, 311–318.
- [3] a) M. Behrens, F. Studt, I. Kasatkin, S. Kuhl, M. Havecker, F. Abild-Pedersen, S. Zander, F. Girgsdies, P. Kurr, B. L. Kniep, M. Tovar, R. W. Fischer, J. K. Norskov, R. Schlögl, *Science* **2012**, *336*, 893–897; b) S. Kuld, M. Thorhauge, H. Falsig, C. F. Elkjaer, S. Helveg, I. Chorkendorff, J. Sehested, *Science* **2016**, *352*, 969–974; c) T. Lunkenbein, J. Schumann, M. Behrens, R. Schlögl, M. G. Willinger, *Angew. Chem. Int. Ed.* **2015**, *54*, 4544–4548; *Angew. Chem.* **2015**, *127*, 4627–4631; d) F. Studt, M. Behrens, E. L. Kunkes, N. Thomas, S. Zander, A. Tarasov, J. Schumann, E. Frei, J. B. Varley, F. Abild-Pedersen, J. K. Norskov, R. Schlögl, *ChemCatChem* **2015**, *7*, 1105–1111; e) S. Zander, E. L. Kunkes, M. E. Schuster, J. Schumann, G. Weinberg, D. Teschner, N. Jacobsen, R. Schlögl, M. Behrens, *Angew. Chem. Int. Ed.* **2013**, *52*, 6536–6540; *Angew. Chem.* **2013**, *125*, 6664–6669; f) S. Kuld, C. Conradsen, P. G. Moses, I. Chorkendorff, J. Sehested, *Angew. Chem. Int. Ed.* **2014**, *53*, 5941–5945; *Angew. Chem.* **2014**, *126*, 6051–6055.

- [4] a) T. Witoon, J. Chalorngtham, P. Dumrongbunditkul, M. Chareonpanich, J. Limtrakul, *Chem. Eng. J.* **2016**, *293*, 327–336; b) F. Frusteri, G. Bonura, C. Cannilla, G. D. Ferrante, A. Aloise, E. Catizzone, M. Migliori, G. Giordano, *Appl. Catal. B* **2015**, *176*, 522–531; c) I. A. Fisher, H. C. Woo, A. T. Bell, *Catal. Lett.* **1997**, *44*, 11–17; d) I. A. Fisher, A. T. Bell, *J. Catal.* **1997**, *172*, 222–237; e) F. Arena, G. Italiano, K. Barbera, S. Bordiga, G. Bonura, L. Spadaro, F. Frusteri, *Appl. Catal. A* **2008**, *350*, 16–23; f) S. Kattel, B. Yan, Y. Yang, J. G. Chen, P. Liu, *J. Am. Chem. Soc.* **2016**, *138*, 12440–12450; g) I. Ro, Y. Liu, M. R. Ball, D. H. K. Jackson, J. P. Chada, C. Sener, T. F. Kuech, R. J. Madon, G. W. Huber, J. A. Dumesic, *ACS Catal.* **2016**, *6*, 7040–7050.
- [5] C. Copéret, A. Comas-Vives, M. P. Conley, D. P. Estes, A. Fedorov, V. Mougél, H. Nagae, F. Nunez-Zarur, P. A. Zhizhko, *Chem. Rev.* **2016**, *116*, 323–421.
- [6] A. Roussey, P. Gentile, D. Lafond, E. Martinez, V. Jousseume, C. Thieuleux, C. Copéret, *J. Mater. Chem. C* **2013**, *1*, 1583–1587.
- [7] E. Guglielminotti, *Langmuir* **1990**, *6*, 1455–1460.
- [8] F. Ouyang, J. N. Kondo, K. Maruya, K. Domen, *Catal. Lett.* **1998**, *50*, 179–181.
- [9] a) O. Syzgantseva, M. Calatayud, C. Minot, *J. Phys. Chem. C* **2010**, *114*, 11918–11923; b) O. A. Syzgantseva, M. Calatayud, C. Minot, *J. Phys. Chem. C* **2012**, *116*, 6636–6644.
- [10] a) K. Mudiyansele, Y. X. Yang, F. M. Hoffmann, O. J. Furlong, J. Hrbek, M. G. White, P. Liu, D. J. Stacchiola, *J. Chem. Phys.* **2013**, *139*, 044712; b) E. M. Mccash, S. F. Parker, J. Pritchard, M. A. Chesters, *Surf. Sci.* **1989**, *215*, 363–377.
- [11] M.-C. Silaghi, A. Comas-Vives, C. Copéret, *ACS Catal.* **2016**, *6*, 4501–4505.
- [12] a) Y. Yang, D. H. Mei, C. H. F. Peden, C. T. Campbell, C. A. Mims, *ACS Catal.* **2015**, *5*, 7328–7337; b) Q. L. Tang, Z. P. Liu, *J. Phys. Chem. C* **2010**, *114*, 8423–8430; c) J. Graciani, K. Mudiyansele, F. Xu, A. E. Baber, J. Evans, S. D. Senanayake, D. J. Stacchiola, P. Liu, J. Hrbek, J. F. Sanz, J. A. Rodriguez, *Science* **2014**, *345*, 546–550; d) M. D. Marcinkowski, C. J. Murphy, M. L. Liriano, N. A. Wasio, F. R. Lucci, E. C. H. Sykes, *ACS Catal.* **2015**, *5*, 7371–7378.
- [13] S. Wesselbaum, V. Moha, M. Meuresch, S. Brosinski, K. M. Thenert, J. Kothe, T. V. Stein, U. Englert, M. Holscher, J. Klankermayer, W. Leitner, *Chem. Sci.* **2015**, *6*, 693–704.

Manuscript received: October 17, 2016

Final Article published: January 23, 2017